Attosecond streaking spectrum in the photoionization of the hydrogen molecular ion

Feng Wang,[1] Kai Liu,[1] Xiaofan Zhang,[1] Zhe Wang,[1] Meiyan Qin,[1] Qing Liao,[1,*] and Peixiang Lu[1,2,†]

[1]*Hubei Key Laboratory of Optical Information and Pattern Recognition, Wuhan Institute of Technology, Wuhan 430205, China*

[2]*Wuhan National Laboratory for Optoelectronics, Huazhong University of Science and Technology, Wuhan 430074, China*

(Received 6 July 2019; published 11 October 2019)

We investigate the attosecond streaking spectrum of H_2^+ by numerically solving the time-dependent Schrödinger equation. The results show that the streaking spectrum of H_2^+ depends sensitively on the internuclear distance R. In addition to the regular streaking structure, some streaking spectra of H_2^+ with the splitting and distorted structures are also observed as R changes. The splitting and distorted streaking spectra of H_2^+ are demonstrated to be related to the destructive two-center interference and resonant transition triggered by the IR field, respectively. Meanwhile, the mixture structure of split and distortion on the streaking spectrum of H_2^+ is attributed to the coupling of the destructive two-center interference and resonant transition. The R-dependent streaking spectra might pave an accessible route toward monitoring the ultrafast nuclear dynamics of molecules.

DOI: 10.1103/PhysRevA.100.043405

I. INTRODUCTION

In the past two decades, fascinating developments in the field of ultrafast optics have stimulated the generation of attosecond pulses [1–3], which provides a powerful tool for probing and controlling the electronic dynamics inside atoms [4–6] and molecules [7,8] and on the surface of metal nanostructures [9–11] with unprecedented resolutions. To date, a number of ultrafast detection techniques based on attosecond pulses have been developed [12–16], among which the attosecond streaking technique is a prominent one [17].

In the attosecond streaking technique, the photoelectron wave packet is created by an attosecond extreme ultraviolet (XUV) pulse and steered by a moderately strong IR field. By recording a set of photoelectron energy spectra (PEESs) over a range of delays between these two pulses, a streaking spectrum is obtained. Since the time structure of the exciting pulse is fully encoded in the released electron wave packets, the streaking spectrum therefore has been widely used for accurate characterization of the attosecond pulse [18–21]. On the other hand, the released electron wave packets carry valuable information about the processes that produced them, and the streaking spectrum has also been applied to monitor the ionization dynamics of electrons [22–27]. For example, Schultze *et al.* measured a small time shift of 21 ± 5 as between the photoemission from $2p$ and $2s$ subshells of atomic neon by the streaking technique [24]. Zhang and Thumm found that the Coulomb-laser coupling effect in a streaking setting of hydrogen atom results in an advanced emission of the electron wave packet relative to the IR field's vector potential [25]. Moreover, the polarization of the initial state [26] and many-electron effects [27] are also demonstrated to be imprinted on the streaking spectrum.

Compared to the atoms, the IR field-assisted photoionization of molecules is more complicated due to the rich internal structure of the molecule [28–33]. Recently, Ning *et al.* found that the destructive Cohen-Fano interferences can lead to an increased streaking time shift in the H_2^+ [32]. Chacón and Ruiz demonstrated that the interference of electron wave packets emitted from the highest occupied and lowest unoccupied molecular orbital will also give rise to a larger streaking time shift in the CO molecule [33]. Except the streaking time shift, the shapes of the streaking spectra intuitively reveal the electron dynamics in the laser-molecule interaction, which, however, has scarcely been investigated.

In this paper, we take the simplest molecule H_2^+ as an example to systematically investigate the features of molecular streaking spectra by numerically solving the time-dependent Schrödinger equation (TDSE). The results show that with the internuclear distance changes the splitting and distorted structures are observed in the streaking spectra of H_2^+. Moreover, at a specific internuclear distance, the splitting and distorted structures coexist in the streaking spectrum. Further analyses indicate that the splitting streaking spectrum originates from the destructive interference of electron wave packets emitted from the two nuclei of H_2^+, while the distorted streaking spectrum is a consequence of the resonant transition from $1s\sigma_g$ to $2p\sigma_u$ states of H_2^+ induced by the IR field. The coexistence of the splitting and distorted structures in the streaking spectrum is due to the coupling of the destructive two-center interference and resonant transition.

II. THEORETICAL MODEL

In this paper, the IR and XUV fields are both linearly polarized along the $\vec{x}$ direction, thus the electron dynamics are mainly confined along the polarization direction. It is reasonable to model the streaking spectrum of H_2^+ by solving

*liaoqing@wit.edu.cn

†lupeixiang@mail.hust.edu.cn

the TDSE in one spatial dimension [34]:

$$i\frac{\partial\Psi(x,t)}{\partial t}=\left[-\frac{1}{2}\frac{\partial^2}{\partial x^2}+V(x)+V_l(x,t)\right]\Psi(x,t), \quad (1)$$

where $V(x)=1/R-1/\sqrt{(x-R/2)^2+1}-1/\sqrt{(x+R/2)^2+1}$ is the soft-core potential of H_2^+, the first term of $V(x)$ is the Coulomb interaction between the two nuclei of H_2^+, the latter two terms of $V(x)$ denote the Coulomb interaction between the electron and the two nuclei, and R is the internuclear distance. In the dipole approximation, the length-gauged laser-molecule interaction can be written as $V_l(x,t)=-E(t)x$. $E(t)$ is the electric field, which is composed by a linearly polarized IR field and an XUV pulse:

$$E(t)=E_{l0}\cos^2(\pi t/T_l)\cos(\omega_l t)+E_{x0}e^{-2In(2)[(t-\tau)/T_x]^2}\cos[\omega_x(t-\tau)]. \quad (2)$$

Here E_{l0} (E_{x0}), ω_l (ω_x), and T_l (T_x) are the amplitude, central frequency, and pulse duration of the IR (XUV) field, respectively. τ is the time delay between these two pulses.

Equation (1) is solved by using the Crank-Nicholson method. The initial wave function is prepared by imaginary-time propagation [35]. The electron wave function $\Psi(x,t)$ is split into two parts at each time step t_i [36]:

$$\Psi(x,t_i)=\Psi_{\rm I}(x,t_i)+\Psi_{\rm II}(x,t_i)=\Psi(x,t_i)[1-F_s(R_s)]+\Psi(x,t_i)F_s(R_s). \quad (3)$$

$F_s(R_s)=1/[1+e^{(|x|-R_s)/\Delta}]$ is a spilt function that separates the whole space into the inner ($0\longrightarrow R_s$) and outer ($R_s\longrightarrow R_{\rm max}$) regions smoothly. Δ is the width of the crossover region and R_s is the boundary of the inner space. In the inner space, $\Psi_{\rm I}(x,t_i)$ propagates under the full Hamiltonian, while in the outer region $\Psi_{\rm II}(x,t_i)$, which denotes the "ionized part," propagates under the Volkov Hamiltonian [37]. Specifically, the ionized wave packet $\Psi_{\rm II}(x,t_i)$ is first transformed into the momentum space $C(\vec{k},t_i)$ at each time step t_i, and then it propagates from time t_i to the end of the laser pulse. The photoelectron momentum distribution (PEMD) is obtained in terms of

$$\frac{dP(\vec{k})}{dE_f}=\sqrt{2E_f}\left|\sum_i\bar{C}(\vec{k},t_i)\right|^2, \quad (4)$$

where $\bar{C}(\vec{k},t_i)=e^{-i\int_{t_i}^{\infty}\frac{1}{2}[\vec{p}+\vec{A}(t_i')]^2dt_i'}C(\vec{k},t_i)$. $E_f=\vec{k}^2/2$ and $\vec{k}$ represent the final energy and momentum of the electron. $\vec{A}(t_i')$ is the total vector potential of the laser fields. By integrating the PEMDs at the different XUV-IR delays, the streaking spectrum of H_2^+ is obtained.

In our simulations, the boundary of the inner space R_s and the width of the crossover region Δ are set to 40 and 2 a.u., respectively. The Cartesian grid ranges from -2300 to 2300 a.u. with a grid size of $\Delta x=0.1$ a.u. The time step of propagation is $\Delta t=0.01$ a.u. At the end of the pulse, the wave function is propagated for an additional few femtoseconds to collect "slow" electrons [38,39].

III. RESULTS AND DISCUSSIONS

We have calculated the streaking spectra of H_2^+ with different internuclear distances R by using a 600-as XUV pulse with the photon energy of 50 eV in combination with a five-cycle, 800-nm IR field. In our simulations, the H_2^+ is assumed to be aligned along the polarization direction of laser pulses. The intensities of XUV and IR fields are 1×10^{12} and 1×10^{11} W/cm^2, respectively. The calculated results show that the streaking spectrum of H_2^+ depends sensitively on the internuclear distance R. Four types of streaking spectra are observed as R varies. The detailed results are discussed in the following subsections.

A. Type 1: Regular structure

The first kind of streaking spectrum is the most common one, which appears at a large majority of the internuclear distances and exhibits a regular streaking structure as shown in Figs. 1(a) and 1(b) for the results of $R=3$ and 7 a.u. In these cases, the single-photon PEES generated by using the XUV pulse shows a Gaussian distribution [see Figs. 1(c) and 1(d)] that is centered at $E_c=\omega_x-I_p$, where I_p is the ionization potential of H_2^+. Note that the ionization potential I_p of H_2^+ decreases with the increase of the internuclear distance [40,41]. Therefore, E_c for $R=7$ a.u. [Fig. 1(d)] is much larger than that for $R=3$ a.u. [Fig. 1(c)]. When subjected to the IR field, the electron ionized at the XUV-IR delay τ by the XUV pulse will be reaccelerated by the IR field and gain extra energy, which is proportional to $A_l(\tau)$ [25]. Here, $A_l(\tau)=\int_{-\infty}^{\tau}E_l(t')dt'$ is the IR field's vector potential at the ionization time τ. As the τ is changed, the center energy E_c of the PEES will oscillate like the time-dependent vector potential of the IR field, thus leading to the regular streaking spectra in Figs. 1(a) and 1(b).

B. Type 2: Splitting structure

The second kind of streaking spectrum is observed at some specific internuclear distances, such as $R=8.5$ a.u. in

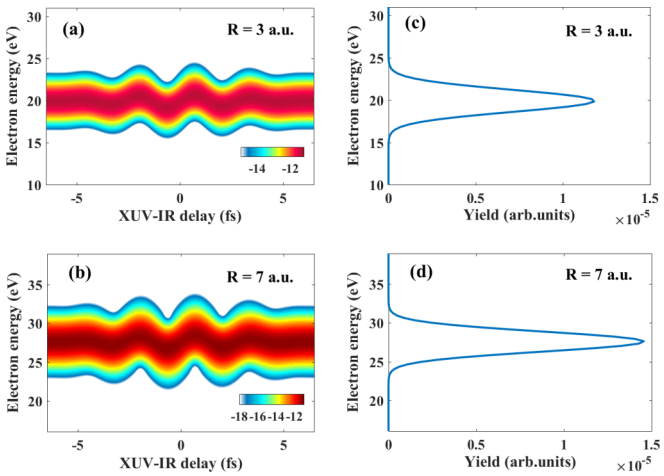

FIG. 1. (a, b) The streaking spectra of H_2^+ by using a 50-eV XUV pulse and a synchronized 800-nm IR field with the intensity of 1×10^{11} W/cm^2. The internuclear distances of H_2^+ are fixed at 3 and 7 a.u., respectively. (c, d) Same as (a) and (b), but for the PEESs by using only the XUV pulse.

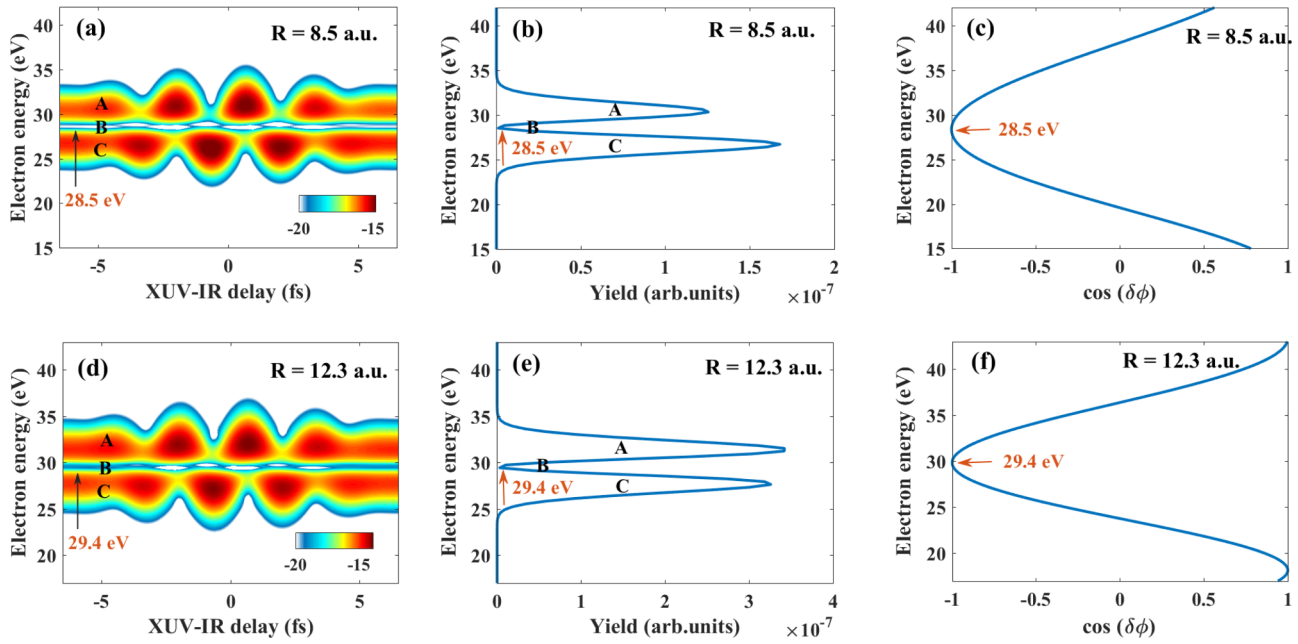

FIG. 2. (a–c) The streaking spectrum, PEES, and predicted position of the photoionization-yield minimum for $R = 8.5$ a.u. (d–f) Same as (a)–(c), but for R of 12.3 a.u.

Fig. 2(a) and $R = 12.3$ a.u. in Fig. 2(d). In these cases, the central parts of streaking spectra are seriously suppressed (marked as B). The obtained streaking spectra are split into up (marked as A) and down (marked as C) parts. To understand this phenomenon, we have calculated the single-photon PEESs with $R = 8.5$ and 12.3 a.u. The results are presented in Figs. 2(b) and 2(e), respectively. One can see that the PEESs in these two cases are also suppressed at the central parts [marked as B in Figs. 2(b) and 2(e); the corresponding photoelectron energy is about 28.5 eV for $R = 8.5$ a.u. and 29.4 eV for $R = 12.3$ a.u.] and exhibit a two-peak structure [marked as A and C in Figs. 2(b) and 2(e)]. These results are consistent with the splitting streaking spectra in Figs. 2(a) and 2(d). For $H_2{}^+$, the ionized electron wave packet can be considered as a coherent superposition of that emitted from the two nuclei. Similar to Young's double-slit interference [42], the photoionization yield is approximately proportional to $[1 + \cos(\delta\phi)]^2$, where $\delta\phi$ is the phase difference of the two electron wave packets emitted from the two nuclei. Based on the eikonal model [43], the phase difference $\delta\phi$ can be derivated as $\delta\phi = \int_{-R/2}^{R/2} p(x)dx$, where $p(x) = \sqrt{2[E_f - V(x)]}$ is the instantaneous momentum of the electron and E_f is the photoelectron energy. Here, the two nuclei are assumed to locate at $(R/2, 0)$ and $(-R/2, 0)$, respectively. In Figs. 2(c) and 2(f), we have calculated the $\cos(\delta\phi)$ as a function of the photoelectron energy E_f for $R = 8.5$ and 12.3 a.u. It is obvious that the destructive interference $[\cos(\delta\phi) = -1]$ occurs at E_f=28.5 eV for $R = 8.5$ a.u. and at E_f=29.4 eV for $R = 12.3$ a.u., which correspond to the minima (marked as B) in the single-photon PEESs and streaking spectra in Figs. 2(a) and 2(b) and in Figs. 2(d) and 2(e), respectively. Note that, since the IR field used in our simulation is very weak, it hardly changes the phase difference $\delta\phi$ or therefore the position of the minimum in the streaking spectrum as the XUV-IR delay varies.

C. Type 3: Distorted structure

Figure 3(a) presents the third kind of streaking spectrum, which appears at $R = 5.5$ a.u. One can see that the streaking spectrum is seriously distorted, especially at $\tau > -4$ fs. To understand this phenomenon, we have also plotted the single-photon PEES for $H_2{}^+$ at $R = 5.5$ a.u. in Fig. 3(b). Like the results in Figs. 1(c) and 1(d), the PEES here also shows a Gaussian distribution. This result indicates that the distortion on the streaking spectrum in Fig. 3(a) should not arise from the single-photon ionization by the XUV pulse, but from the interaction with the IR field. We note that the photon energy of the IR field is very close to the energy difference between the $1s\sigma_g$ and $2p\sigma_u$ states of $H_2{}^+$ when $R = 5.5$ a.u. [see Fig. 3(c)]. Thus, a resonant transition from the $1s\sigma_g$ to $2p\sigma_u$ states will possibly occur through the absorption of one IR photon ω_l [see black arrows in Fig. 3(c)]. Such a resonant transition will lead to a superposition of the $1s\sigma_g$ and $2p\sigma_u$ states of H_2^+. The interference of the electron wave packets emitted from these two states could therefore give rise to the distorted structures in the streaking spectrum. To verify the above analysis, we have calculated the time-dependent populations of the $1s\sigma_g$ and $2p\sigma_u$ states of $H_2{}^+$ in the IR field. In our calculations, the populations of the $1s\sigma_g$ and $2p\sigma_u$ states are obtained by $|\langle\psi_{s,p}(x)|\Psi(x,t)\rangle|^2$. Here $\Psi(x,t)$ is the time-dependent wave function driven by the IR field alone. $\psi_{s,p}(x)$ represents the wave function of the $1s\sigma_g$ and $2p\sigma_u$ states of $H_2{}^+$, respectively. As shown in Fig. 3(d), the population of the $2p\sigma_u$ state (green solid line) is gradually increased after $t = -4$ fs; meanwhile, the population of the $1s\sigma_g$ state (orange solid line) is decreased, meaning that the IR field induces a transition between these two states. Furthermore, we have calculated the relative phase $\delta\vartheta$ of the wave functions from the $1s\sigma_g$ and $2p\sigma_u$ states, which is given by $\delta\vartheta = \vartheta_s - \vartheta_p$ with $\vartheta_{s,p} = \arg[\langle\psi_{s,p}(x)|\Psi(x,t)\rangle]$. As can be seen from Fig. 3(e), the oscillation of delay-dependent

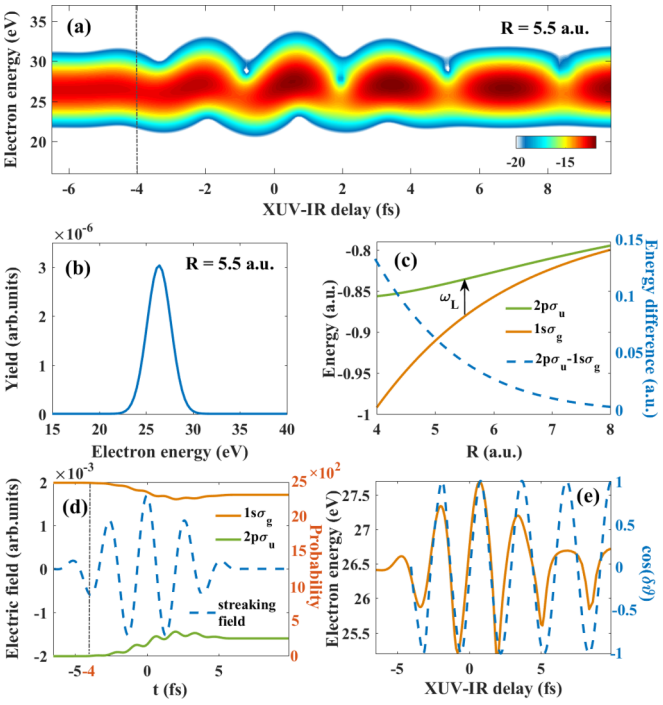

FIG. 3. (a, b) The streaking spectrum and PEES for $R = 5.5$ a.u. (c) Energy levels of the $1s\sigma_g$ and $2p\sigma_u$ states of H_2^+. The blue dashed line indicates the energy difference between the $1s\sigma_g$ and $2p\sigma_u$ states. (d) Populations on the $1s\sigma_g$ and $2p\sigma_u$ states as a function of time. The blue dashed line indicates the IR streaking field. (e) The orange solid line indicates the center energies E_c (τ) of the streaking spectrum in Fig. 3(a). The blue dashed line indicates $\cos(\delta\vartheta)$, where $\delta\vartheta$ is the relative phase of the $1s\sigma_g$ and $2p\sigma_u$ states in H_2^+ obtained by using only the IR streaking field.

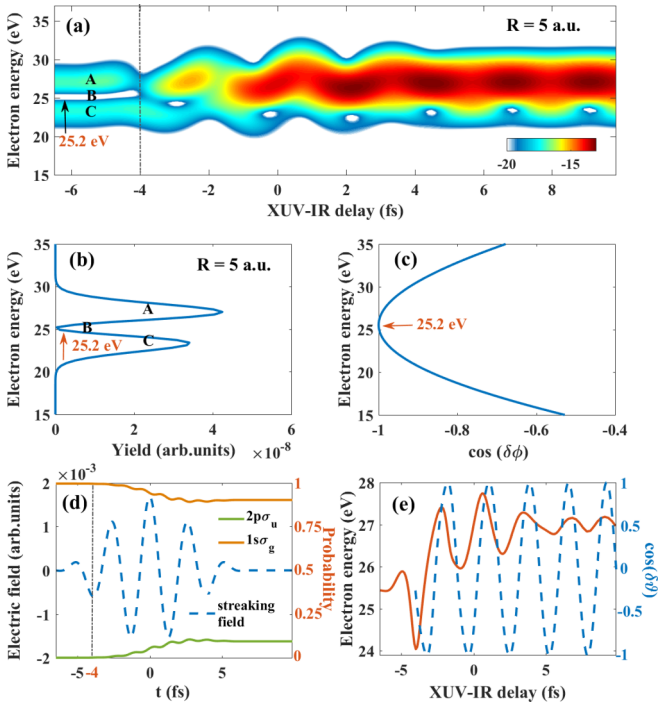

FIG. 4. (a–c) The streaking spectrum, PEES, and predicted position of the photoionization-yield minimum for $R = 5$ a.u. (d) Populations on the $1s\sigma_g$ and $2p\sigma_u$ states as a function of time. The blue dashed line indicates the IR streaking field. (e) The orange solid line indicates the center energies E_c (τ) of the streaking spectrum in Fig. 4(a). The blue dashed line indicates $\cos(\delta\vartheta)$.

center energies E_c (τ) (orange solid line) of the streaking spectrum matches well with $\cos(\delta\vartheta)$ (blue dashed line). Such an agreement indicates that the distorted streaking spectrum in Fig. 3(a) is indeed a consequence of the resonant transition between the $1s\sigma_g$ and $2p\sigma_u$ states triggered by the IR field.

D. Type 4: Mixture of the splitting and distorted structures

In Fig. 4(a), we show the fourth kind of streaking spectrum, observed at $R = 5$ a.u. In this case, the streaking spectrum presents a splitting structure at $\tau < -4$ fs and a distorted structure at $\tau > -4$ fs. Likewise, we have also calculated the single-photon PEES for H_2^+ at $R = 5$ a.u. The result is shown in Fig. 4(b). Similar to the results in Figs. 2(b) and 2(e), the obtained PEES also shows a two-peak structure [marked as A and C in Fig. 4(b)]. The splitting streaking spectrum at $\tau < -4$ fs in Fig. 4(a) thus can be understood as a consequence of the two-center interference effect as Type 2 in Fig. 2. Further evidence can be found in Fig. 4(c), which shows our simulations based on the eikonal model [43]. One can see that the destructive interference $[\cos(\delta\phi) = -1]$ occurs at $E_f = 25.2$ eV, which corresponds to the minima (marked as B) in the single-photon PEES and streaking spectrum in Figs. 4(a) and 4(b). For the distorted structure at $\tau > -4$ fs, it can also be related to the resonant transition effect induced by the IR field, since the energy difference (0.066 eV) between the $1s\sigma_g$ and $2p\sigma_u$ states of H_2^+ at $R = 5$ a.u is also close to the photon energy of the IR field (0.057 eV). To check this point, we have plotted the time-dependent populations of the $1s\sigma_g$ to $2p\sigma_u$ states in Fig. 4(d). It is clear that the electron wave packet is partly transferred from the $1s\sigma_g$ (orange solid line) to $2p\sigma_u$ state (green solid line) at $t > -4$ fs. The interference of the wave functions from these two states will therefore lead to the distorted structures as discussed in Fig. 3. This can also be confirmed from Fig. 4(e), which shows relative phase $\delta\vartheta$ between the wave functions from the $1s\sigma_g$ to $2p\sigma_u$ states as well as the delay-dependent center energy E_c (τ) of the streaking spectrum. The oscillation behavior of E_c (τ) (orange solid line) is very similar to that of the $\cos(\delta\vartheta)$ (blue dashed line). Note that at $\tau < -4$ fs the $2p\sigma_u$ state is hardly populated, thus the streaking spectrum structure is mainly affected by the two-center interference effect, while for $\tau > -4$ fs the resonant transition effect becomes dominant.

IV. CONCLUSION

In conclusion, we have investigated the streaking spectra of H_2^+ by numerically solving the TDSE. We find that in our laser conditions the streaking spectrum of H_2^+ depends sensitively on the internuclear distance R and four types of streaking spectra are observed as R varies. The first kind is the conventional streaking spectrum, which exhibits a regular streaking structure and appears at a large majority of internuclear distances. The second kind of streaking spectrum is observed at the internuclear distances like $R = 8.5$ and

12.3 a.u., which presents a splitting structure. Based on the eikonal model, the splitting structure in the streaking spectrum is demonstrated to originate from the destructive interference of electron wave packets emitted from the two nuclei of H_2^+. At $R = 5.5$ a.u., we discover the third kind of streaking spectrum with a distorted structure, which is demonstrated to be a consequence of the resonant transition from $1s\sigma_g$ to $2p\sigma_u$ states of H_2^+ induced by the IR field. Moreover, due to the coupling of the destructive two-center interference and resonant transition, the fourth kind of streaking spectrum, i.e., a mixture of the splitting and distorted structures on the streaking spectrum, is also found at $R = 5$ a.u. The R-dependent streaking spectra will provide a valuable guideline for monitoring the ultrafast nuclear dynamics of molecules.

ACKNOWLEDGMENTS

This work was supported by National Natural Science Foundation of China under Grants No. 11934006, No. 11674257, and No. 11604248 and the Program for Distinguished Middle-Aged and Young Innovative Research Team in Higher Education of Hubei, China (Grant No. T201806).

[1] F. Krausz and M. Ivanov, Rev. Mod. Phys. **81**, 163 (2009).
[2] P. Lan, P. Lu, W. Cao, Y. Li, and X. Wang, Phys. Rev. A **76**, 051801(R) (2007); H. Yuan, L. He, F. Wang, B. Wang, W. Liu, and Z. Hong, Opt. Quantum Electron **49**, 214 (2017).
[3] J. Li, X. Ren, Y. Yin, K. Zhao, A. Chew, Y. Cheng, E. Cunningham, Y. Wang, S. Hu, Y. Wu, M. Chini, and Z. Chang, Nat. Commun. **8**, 186 (2017).
[4] M. F. Kling and M. J. J. Vrakking, Annu. Rev. Phys. Chem **59**, 463 (2008).
[5] J. Tan, Y. Zhou, M. He, Y. Chen, Q. Ke, J. Liang, X. Zhu, M. Li, and P. Lu, Phys. Rev. Lett. **121**, 253203 (2018); M. Li, H. Xie, W. Cao, S. Luo, J. Tan, Y. Feng, B. Du, W. Zhang, Y. Li, Q. Zhang, P. Lan, Y. Zhou, and P. Lu, *ibid.* **122**, 183202 (2019); Y. Liu, J. Tan, M. He, H. Xie, Y. Qin, Y. Zhao, M. Li, Y. Zhou, and P. Lu, Opt. Quantum Electron **51**, 145 (2019); S. Luo, M. Li, W. Xie, K. Liu, Y. Feng, B. Du, Y. Zhou, and P. Lu, Phys. Rev. A **99**, 053422 (2019).
[6] M. Th. Hassan, T. T. Luu, A. Moulet, O. Raskazovskaya, P. Zhokhov, M. Garg, N. Karpowicz, A. W. Zheltikov, V. Pervak, F. Krausz, and E. Goulielmakis, Nature (London) **530**, 66 (2016).
[7] Ch. Neidel, J. Klei, C.-H. Yang, A. Rouzée, M. J. J. Vrakking, K. Klünder, M. Miranda, C. L. Arnold, T. Fordell, A. L'Huillier, M. Gisselbrecht, P. Johnsson, M. P. Dinh, E. Suraud, P. G. Reinhard, V. Despré, M. A. L. Marques, and F. Lépine, Phys. Rev. Lett. **111**, 033001 (2013).
[8] Y. He, L. He, P. Lan, B. Wang, L. Li, X. Zhu, W. Cao, and P. Lu, Phys. Rev. A **99**, 053419 (2019); Y. N. Qin, M. Li, Y. Li, M. He, S. Luo, Y. Liu, Y. Zhou, and P. Lu, *ibid.* **99**, 013431 (2019).
[9] M. I. Stockman, M. F. Kling, U. Kleineberg, and F. Krausz, Nat. Photon. **1**, 539 (2007).
[10] Q. Liao and U. Thumm, Phys. Rev. Lett. **112**, 023602 (2014); L. Li, P. Lan, X. Zhu, T. Huang, Q. Zhang, M. Lein, and P. Lu, *ibid.* **122**, 193901 (2019); L. Li, P. Lan, L. He, W. Cao, Q. Zhang, and P. Lu, arXiv:1908.07283.
[11] J. Li, Q. Zhang, L. Li, X. Zhu, T. Huang, P. Lan, and P. Lu, Phys. Rev. A **99**, 033421 (2019); S. Ke, D. Zhao, J. Liu, Q. Liu, Q. Liao, B. Wang, and P. Lu, Opt. Express **27**, 13858 (2019); D. M. Kinyua, H. Long, X. Xing, S. Njoroge, K. Wang, B. Wang and P. Lu, Nanotechnology **30**, 305201 (2019).
[12] L. Gallmann, C. Cirelly, and U. Keller, Annu. Rev. Phys. Chem. **63**, 447 (2012).
[13] K. Klünder, J. M. Dahlström, M. Gisselbrecht, T. Fordell, M. Swoboda, D. Guénot, P. Johnsson, J. Caillat, J. Mauritsson, A. Maquet, R. Taïeb, and A. L'Huillier, Phys. Rev. Lett. **106**, 143002 (2011).
[14] A. N. Pfeiffer, C. Cirelli, M. Smolarski, R. Dörner, and U. Keller, Nat. Phys. **7**, 428 (2011).
[15] D. Kiesewetter, R. R. Jones, A. Camper, S. B. Schoun, P. Agostini, and L. F. Dimauro, Nat. Phys. **14**, 68 (2018).
[16] C. Zhai, Y. Zhang, and Q. Zhang, Opt. Communication **437**, 104 (2019).
[17] J. Itatani, F. Quéré, G. L. Yudin, M. Y. Ivanov, F. Krausz, and P. B. Corkum, Phys. Rev. Lett. **88**, 173903 (2002).
[18] Y. Mairesse and F. Quéré, Phys. Rev. A **71**, 011401(R) (2005).
[19] T. Gaumnitz, A. Jain, and H. J. Wörner, Opt. Express **26**, 14719 (2018).
[20] F. Quéré, J. Itatani, G. L. Yudin, and P. B. Corkum, Phys. Rev. Lett. **90**, 073902 (2003).
[21] F. Wang, K. Liu, M. Qin, Q. Liao, P. Lan, and P. Lu, J. Opt. Soc. Am. B **36**, 7 (2019).
[22] M. Isinger, R. J. Squibb, D. Busto, S. Zhong, A. Harth, D. Kroon, S. Nandi, C. L. Arnold, M. Miranda, J. M. Dahlström, E. Lindroth, R. Feifel, M. Gisselbrecht, and A. L'Huillier, Science **358**, 893 (2017).
[23] O. Smirnova, A. S. Mouritzen, S. Patchkovskii, and M. Y. Ivanov, J. Phys. B **40**, F197 (2007).
[24] M. Schultze, M. Fie, N. Karpowicz, J. Gagnon, M. Korbman, M. Hofstetter, S. Neppl, A. L. Cavalieri, Y. Komninos *et al.*, Science **328**, 1658 (2010).
[25] C.-H. Zhang and U. Thumm, Phys. Rev. A **82**, 043405 (2010).
[26] R. Pazourek, S. Nagele, K. Doblhoff-Dier, J. Feist, C. Lemell, K. Tőkési, and J. Burgdörfer, J. Phys. Conf. Ser. **388**, 012029 (2012).
[27] D. Hochstuhl and M. Bonitz, Phys. Rev. A **86**, 053424 (2012).
[28] V. V. Serov, V. L. Derbov, and T. A. Sergeeva, Phys. Rev. A **87**, 063414 (2013).
[29] S. Kawai and A. D. Bandrauk, Phys. Rev. A **75**, 063402 (2007).
[30] S. Haessler, B. Fabre, J. Higuet, J. Caillat, T. Ruchon, P. Breger, B. Carré, E. Constant, A. Maquet, E. Mével, P. Salières, R. Taïeb, and Y. Mairesse, Phys. Rev. A **80**, 011404(R) (2009).
[31] A. L. D. Kilcoyne, A. Aguilar, A. Müller, S. Schippers, C. Cisneros, G. Alna'Washi, N. B. Aryal, K. K. Baral, D. A. Esteves, C. M. Thomas, and R. A. Phaneuf, Phys. Rev. Lett. **105**, 213001 (2010).
[32] Q.-C. Ning, L.-Y. Peng, S.-N. Song, W.-C. Jiang, S. Nagele, R. Pazourek, J. Burgdörfer, and Q. Gong, Phys. Rev. A **90**, 013423 (2014).

[33] A. Chacón and C. Ruiz, Opt. Express **26**, 4548 (2018).
[34] C. Yu, H. He, Y. Wang, Q. Shi, Y. Zhang, and R. Lu, J. Phys. B **47**, 055601 (2014).
[35] M. Protopapas, C. H. Keitel, and P. L. Knight, Rep. Prog. Phys. **60**, 389 (1997).
[36] X. M. Tong, K. Hino, and N. Toshima, Phys. Rev. A **74**, 031405(R) (2006).
[37] X. M. Tong, S. Watahiki, K. Hino, and N. Toshima, Phys. Rev. Lett. **99**, 093001 (2007).
[38] P. L. He, N. Takemoto, and F. He, Phys. Rev. A **91**, 063413 (2015); Y. Zhao, Y. Zhou, J. Liang, Z. Zeng, Q. Ke, Y. Liu, M. Li, and P. Lu, Opt. Express **27**, 21689 (2019).
[39] J. Tan, Y. Zhou, M. He, Q. Ke, J. Liang, Y. Li, M. Li, and P. Lu, Phys. Rev. A **99**, 033402 (2019); J. Tan, Y. Li, Y. Zhou, M. He, Y. Chen, M. Li, and P. Lu, Opt. Quantum Electron **50**, 57 (2018); K. Liu, M. Qin, Q. Li, and Q. Liao, *ibid.* **50**, 364 (2018).
[40] T. Zuo, S. Chelkowski, and A. D. Bandrauk, Phys. Rev. A **48**, 3837 (1993).
[41] L. He, Q. Zhang, P. Lan, W. Cao, X. Zhu, C. Zhai, F. Wang, W. Shi, M. Li, X.-B. Bian, Nat. Commum. **9**, 1108 (2018); B. Wang, L. He, Y. Qing, Y. Zhang, R. Shao, P. Lan, and P. Lu, Opt. Express **27**, 30172 (2019).
[42] H. D. Cohen and U. Fano, Phys. Rev. **150**, 30 (1966).
[43] L. I. Schiff, *Quantum Mechanics* (McGraw-Hill, New York, 1968).